

Radiative type-I seesaw model with dark matter via $U(1)_{B-L}$ gauge symmetry breaking at future linear colliders

Shinya Kanemura,^{1,*} Takehiro Nabeshima,^{1,†} and Hiroaki Sugiyama^{1,‡}

¹ *Department of Physics, University of Toyama, Toyama 930-8555, Japan*

Abstract

We discuss phenomenology of the radiative seesaw model in which spontaneous breaking of the $U(1)_{B-L}$ gauge symmetry at the TeV scale gives the common origin for masses of neutrinos and dark matter [1]. In this model, the stability of dark matter is realized by the global $U(1)_{DM}$ symmetry which arises by the B–L charge assignment. Right-handed neutrinos obtain TeV scale Majorana masses at the tree level. Dirac masses of neutrinos are generated via one-loop diagrams. Consequently, tiny neutrino masses are generated at the two-loop level by the seesaw mechanism. This model gives characteristic predictions, such as light decayable right-handed neutrinos, Dirac fermion dark matter and an extra heavy vector boson. These new particles would be accessible at collider experiments because their masses are at the TeV scale. The $U(1)_{B-L}$ vector boson may be found at the LHC, while the other new particles could only be tested at future linear colliders. We find that the dark matter can be observed at a linear collider with $\sqrt{s}=500$ GeV and that light right-handed neutrinos can also be probed with $\sqrt{s}=1$ TeV.

PACS numbers: 95.35.+d, 12.60.Cn, 14.60.St

*Electronic address: kanemu@sci.u-toyama.ac.jp

†Electronic address: nabe@jodo.sci.u-toyama.ac.jp

‡Electronic address: sugiyama@sci.u-toyama.ac.jp

I. INTRODUCTION

The standard model of elementary particle physics (SM) is a very successful model which explains $\mathcal{O}(100)$ GeV physics. However, we must consider beyond the SM because several phenomena such as neutrino oscillation [2–7], dark matter (DM) [8, 9] and baryon asymmetry of Universe [10] cannot be explained by the SM.

The neutrino oscillation can be explained by tiny neutrino masses. The simplest method to obtain these masses is the seesaw mechanism [11] with right-handed Majorana neutrinos (the type-I seesaw scenario). In this mechanism, right-handed neutrino masses are $\mathcal{O}(10^{15})$ GeV for $\mathcal{O}(1)$ neutrino Dirac Yukawa couplings. However, these heavy right-handed neutrinos would be difficult to detected at future experiments. On the other hand, if tiny neutrino masses are generated at the loop level, new particle masses can be $\mathcal{O}(1)$ TeV with sizable coupling constants. Moreover, this mechanism is often applied to the models with the Z_2 parity or an $U(1)$ symmetry to forbid tree-level neutrino masses and to guarantee the stability of dark matter [1, 12–25]. If dark matter is a Weakly Interacting Massive Particle (WIMP), its mass is naively estimated to be of $\mathcal{O}(100\text{--}1000)$ GeV by the WMAP data [9]. Such a mass scale for the dark matter may be naturally generated by the vacuum expectation value with respect to the spontaneous break down at the TeV-scale of an additional gauge symmetry.

Let us consider the radiative seesaw model in which spontaneous breaking of the $U(1)_{B-L}$ gauge symmetry at the TeV scale gives the common origin for masses of neutrinos and dark matter [1]. In this model, the stability of dark matter is realized by the global $U(1)_{DM}$ symmetry which arises by B–L charge assignment. In this model, right-handed neutrinos obtain TeV-scale Majorana masses at the tree level, while Dirac masses of neutrinos are generated via one-loop diagrams where the dark matter is running in the loop. Consequently, tiny neutrino masses are generated at the two-loop level by the seesaw mechanism. This model gives characteristic predictions, such as light decayable right-handed neutrinos, Dirac fermion WIMP dark matter and an extra heavy vector boson with the mass to be the TeV scale. These new particles would be accessible at collider experiments so that the model would be testable. For example, the LHC may be able to detect the $U(1)_{B-L}$ gauge boson (Z') with the mass up to about 4 TeV with the $U(1)_{B-L}$ gauge coupling constant about 0.1 [29]. However, it would be challenging to test the other new particles in this model at the LHC unless the Z' boson is sufficiently light, because they only couple to the Z' boson and leptons so that their discovery strongly depends on the mass of the Z' boson.

In this paper, we discuss a possibility of testing this model at future electron-positron linear colliders [30, 31]. Differently from the hadron collider, new Dirac fermions can be produced directly from the e^+e^- collision, whose sequential decays can contain production

Particles	s^0	η	Ψ_{Ri}	Ψ_{Li}	ν_{Ri}	σ^0
SU(3) _C	<u>1</u>	<u>1</u>	<u>1</u>	<u>1</u>	<u>1</u>	<u>1</u>
SU(2) _L	<u>1</u>	<u>2</u>	<u>1</u>	<u>1</u>	<u>1</u>	<u>1</u>
U(1) _Y	0	1/2	0	0	0	0
U(1) _{B-L}	1/2	1/2	-1/2	3/2	1	2

TABLE I: New particles and their quantum charges.

of right-handed neutrinos with the dark matter. The dark matter can also be directly produced in association with charged inert scalar bosons from leptons. We find that for the center-of-mass energy being $\sqrt{s} = 350$ GeV with the integrated luminosity of 1 ab^{-1} , the Dirac fermion dark matter can be detected as long as its mass is less than about 64 GeV. For the center-of-mass energy $\sqrt{s} = 500$ GeV with the same luminosity, the dark matter with the mass of $\mathcal{O}(100)$ GeV can be detected. Moreover, at the linear collider with $\sqrt{s} = 1$ TeV with 3 ab^{-1} right-handed neutrinos can be tested. Therefore, this model can be identified by the combination of these future experiments.

This paper is organized as follows. In the next section, we introduce the radiative type-I seesaw model. We discuss prospect at the LHC in Sec.3 and the ILC in Sec.4. Conclusions are given in Sec.5.

II. THE RADIATIVE TYPE-I SEESAW MODEL

We consider the TeV-scale seesaw model which explains tiny neutrino masses, the dark matter mass and the stability of the dark matter via the $U(1)_{B-L}$ gauge symmetry breaking [1]. New particles and their gauge charges are shown in Table I. Here, s^0, η and σ^0 are complex scalar fields while ν_{Ri}, Ψ_{Ri} and Ψ_{Li} ($i = 1, 2$) are Weyl fermions. This model has $U(1)_{B-L}$ anomalies but those anomalies can be cancelled by new fermions whose masses are larger than $\mathcal{O}(10)$ TeV.

Yukawa interactions are given by

$$\begin{aligned}
\mathcal{L}_{\text{Yukawa}} = & \mathcal{L}_{\text{SM-Yukawa}} - y_{Ri} \overline{(\nu_{Ri})^c} \nu_{Ri} (\sigma^0)^* - y_{\Psi_i} \overline{\Psi_{Ri}} \Psi_{Li} (\sigma^0)^* \\
& - (y_3)_{ij} \overline{(\nu_{Ri})^c} \Psi_{Rj} (s^0)^* - h_{ij} \overline{\Psi_{Li}} \nu_{Rj} s^0 \\
& - f_{\ell i} \overline{L_{L\ell}} \Psi_{Ri} i\sigma_2 \eta^* + \text{h.c.},
\end{aligned} \tag{1}$$

where $\mathcal{L}_{\text{SM-Yukawa}}$ denotes Yukawa interactions of the SM and $L_{L\ell}$ is the left-handed lepton doublet of ℓ ($\ell = e, \mu, \tau$) flavor. Masses of ν_R, Ψ_R and Ψ_L are forbidden by the $U(1)_{B-L}$

gauge symmetry. We take a basis where Yukawa matrices y_R and y_Ψ are diagonalized such that their real positive eigenvalues satisfy $y_{R1} \leq y_{R2}$ and $y_{\Psi_1} \leq y_{\Psi_2}$.

Scalar potential is given by

$$\begin{aligned}
V(\Phi, s, \eta, \sigma) = & -\mu_\phi^2 \Phi^\dagger \Phi + \mu_s^2 |s^0|^2 + \mu_\eta^2 \eta^\dagger \eta - \mu_\sigma^2 |\sigma^0|^2 \\
& + \lambda_\phi (\Phi^\dagger \Phi)^2 + \lambda_s |s^0|^4 + \lambda_\eta (\eta^\dagger \eta)^2 + \lambda_\sigma |\sigma^0|^4 \\
& + \lambda_{s\eta} |s^0|^2 \eta^\dagger \eta + \lambda_{s\phi} |s^0|^2 \Phi^\dagger \Phi + \lambda_{\phi\phi} (\eta^\dagger \eta) (\Phi^\dagger \Phi) + \lambda_{\eta\phi} (\eta^\dagger \Phi) (\Phi^\dagger \eta) \\
& + \lambda_{s\sigma} |s^0|^2 |\sigma^0|^2 + \lambda_{\sigma\eta} |\sigma^0|^2 \eta^\dagger \eta + \lambda_{\sigma\phi} |\sigma^0|^2 \Phi^\dagger \Phi + (\mu_3 s^0 \eta^\dagger \Phi + \text{h.c.}),
\end{aligned} \tag{2}$$

where Φ is the SM Higgs doublet field and μ_ϕ^2 , μ_σ^2 , μ_s^2 , and μ_η^2 are positive values. In our model, there appears global $U(1)$ symmetry (we name it the $U(1)_{DM}$) under which s^0 , η , Ψ_{Ri} and Ψ_{Li} have the same charge. The $U(1)_{DM}$ symmetry stabilizes the dark matter. After the breakings of the $U(1)_{B-L}$ and electroweak symmetries, σ^0 and ϕ^0 obtain vevs $v_\sigma [= \sqrt{2}\langle\sigma^0\rangle]$ and $v [= \sqrt{2}\langle\phi^0\rangle \simeq 246 \text{ GeV}]$, respectively. The $U(1)_{B-L}$ gauge boson Z' acquires its mass as $m_{Z'} = 2g_{B-L}v_\sigma$, where g_{B-L} denotes the gauge coupling constant of the $U(1)_{B-L}$.

Right-handed neutrinos ν_{Ri} obtain Majorana masses $M_{Ri} [= \sqrt{2}y_{Ri}v_\sigma]$ while Ψ_{Ri} and Ψ_{Li} for each i become a Dirac fermion Ψ_i with its mass $M_{\Psi_i} [= y_{\Psi_i}v_\sigma/\sqrt{2}]$. Since the global $U(1)_{DM}$ is not broken by v_σ , the lightest $U(1)_{DM}$ -charged particle is stable. We assume Ψ_1 to be lightest $U(1)_{DM}$ particle and it becomes a candidate for the dark matter.

After symmetry breaking with v_σ and v , mass eigenstates of two CP-even scalars and their mixing angle α are given by

$$\begin{pmatrix} h^0 \\ H^0 \end{pmatrix} = \begin{pmatrix} \cos \alpha & -\sin \alpha \\ \sin \alpha & \cos \alpha \end{pmatrix} \begin{pmatrix} \phi_r^0 \\ \sigma_r^0 \end{pmatrix}, \quad \sin 2\alpha = \frac{2\lambda_{\sigma\phi}vv_\sigma}{m_{H^0}^2 - m_{h^0}^2}, \tag{3}$$

where $\sigma^0 = (v_\sigma + \sigma_r^0 + iz_\sigma)/\sqrt{2}$ and $\phi^0 = (v + \phi_r^0 + iz_\phi)/\sqrt{2}$, and z_ϕ and z_σ are Nambu-Goldstone bosons absorbed by Z and Z' , respectively. Masses of h^0 and H^0 are defined by

$$\begin{aligned}
m_{h^0}^2 &= \lambda_\phi v^2 + \lambda_\sigma v_\sigma^2 - \sqrt{(\lambda_\phi v^2 - \lambda_\sigma v_\sigma^2)^2 + \lambda_{\sigma\phi}^2 v^2 v_\sigma^2}, \\
m_{H^0}^2 &= \lambda_\phi v^2 + \lambda_\sigma v_\sigma^2 + \sqrt{(\lambda_\phi v^2 - \lambda_\sigma v_\sigma^2)^2 + \lambda_{\sigma\phi}^2 v^2 v_\sigma^2}.
\end{aligned} \tag{4}$$

On the other hand, since s^0 and η^0 are $U(1)_{DM}$ -charged particles, they are not mixed with σ^0 and ϕ^0 . Mass eigenstates of these $U(1)_{DM}$ -charged scalars and their mixing angle θ are obtained as

$$\begin{pmatrix} s_1^0 \\ s_2^0 \end{pmatrix} = \begin{pmatrix} \cos \theta & -\sin \theta \\ \sin \theta & \cos \theta \end{pmatrix} \begin{pmatrix} \eta^0 \\ s^0 \end{pmatrix}, \quad \sin 2\theta = \frac{\sqrt{2}\mu_3 v}{m_{s_2^0}^2 - m_{s_1^0}^2}. \tag{5}$$

$f_{\ell i}$	$\begin{pmatrix} 0.0757 & 0.0445 \\ 0.01 & -0.0123 \\ -0.141 & -0.0101 \end{pmatrix}$
h_{ij}	$\begin{pmatrix} -0.131 & 0.1 \\ 0.1 & 0.1 \end{pmatrix}$
$(y_3)_{ij}$	$\begin{pmatrix} 0.0152 & 0.0152 \\ 0.0152 & 0.0152 \end{pmatrix}$
$M_R \equiv M_{R1} = M_{R2}$	250 GeV
$\{M_{\Psi_1}, M_{\Psi_2}\}$	{57.5 GeV, 800 GeV}
$\{m_{h^0}, m_{H^0}, \cos \alpha\}$	{125 GeV, 130 GeV, $1/\sqrt{2}$ }
$\{m_{s_1^0}, m_{s_2^0}, \cos \theta\}$	{200 GeV, 300 GeV, 0.05}
m_{η^\pm}	280 GeV
g_{B-L}	0.1
$m_{Z'}$	4000 GeV

TABLE II: The parameter set which satisfies current experimental bounds. Our analysis is insensitive to the Higgs boson masses m_{h^0} and m_{H^0} .

Mass eigenvalues $m_{s_1^0}$ and $m_{s_2^0}$ of these neutral complex scalars are defined by

$$\begin{aligned}
m_{s_1^0}^2 &= \frac{1}{2} \left(m_\eta^2 + m_s^2 - \sqrt{(m_\eta^2 - m_s^2)^2 + 2\mu_3^2 v^2} \right), \\
m_{s_2^0}^2 &= \frac{1}{2} \left(m_\eta^2 + m_s^2 + \sqrt{(m_\eta^2 - m_s^2)^2 + 2\mu_3^2 v^2} \right),
\end{aligned} \tag{6}$$

where $m_s^2 = \mu_s^2 + \lambda_{s\phi} v_\phi^2/2 + \lambda_{s\sigma} v_\sigma^2/2$ and $m_\eta^2 = \mu_\eta^2 + (\lambda_{\phi\phi} + \lambda_{\eta\phi}) v_\phi^2/2 + \lambda_{\sigma\eta} v_\sigma^2/2$. Finally, the mass of the charged scalar η^\pm is given by

$$m_{\eta^\pm}^2 = \mu_\eta^2 + \lambda_{\phi\phi} \frac{v^2}{2} + \lambda_{\sigma\eta} \frac{v_\sigma^2}{2}. \tag{7}$$

In Table II, we show an examples for the parameter set which satisfies current experimental bounds such as neutrino oscillation, $\mu \rightarrow e\gamma$ constraint, relic abundance of dark matter and dark matter direct detection [1]. We define M_R as a common mass of two ν_{Ri} ($i = 1, 2$).

III. PHYSICS AT THE LHC

We first consider testability of the model at the LHC. We discuss physics of Higgs bosons (h^0 and H^0), the $U(1)_{B-L}$ gauge boson Z' , and the right-handed neutrinos ν_R .

A. Detectability of h and H

Our model predicts two SM-like CP-even Higgs bosons h^0 and H^0 because a large mixing angle between h^0 and H^0 is required to be consistent with the dark matter abundance [1].

In the SM, the Higgs boson mass except for the small region between 122.5 GeV and 127 GeV has already been excluded by the recent LHC results [26, 27]. However, in our model, we can read off from the SM Higgs boson search results that wider regions for m_{h^0} and m_{H^0} remain allowed; i.e., between 110 GeV and 130 GeV, because production cross sections for h^0 and H^0 are reduced by the factor with maximal mixing (1/2) from the SM predictions.

When more data will be accumulated at the LHC, the allowed region will be smaller. Then, only the case with approximately degenerated masses may be allowed, where the two resonances are overlapped and look like one resonance of only one SM Higgs boson depending on the resolution of detectors. If the mass difference is larger than about 1 GeV, the two resonances can be separated at the LHC [26, 27]. Even if the mass difference is smaller, they could be separated at the ILC where the mass can be reconstructed with much better accuracy with the error of $\Delta m \sim 50$ MeV [28].

B. Detectability of Z'

Detectability of the $U(1)_{B-L}$ gauge boson Z' at the LHC has been studied in several papers [29, 32, 33]. The most efficient process of production of the Z' at the LHC is the Drell-Yan mode $q\bar{q} \rightarrow Z'$ where q is a quark in the proton [29, 32, 33]. The Z' boson does not mix with the SM Z boson at the tree level. Therefore, branching ratios of the Z' boson decay are proportional to $U(1)_{B-L}$ charges of daughter particles. The $q\bar{q} \rightarrow Z' \rightarrow \mu^-\mu^+$ process is useful to detect the Z' at the LHC. By using this process, the Z' boson can be detected at the 3σ Confidence Level (C.L.) for $m_{Z'} \lesssim 4$ TeV with $U(1)_{B-L}$ gauge coupling constant $g_{B-L} \simeq 0.1$ at the LHC with $\sqrt{s} = 14$ TeV and 100 fb^{-1} [29]. Essentially, the Z' boson can be distinguished from the other gauge bosons by checking the ratio of $Z' \rightarrow \mu^-\mu^+$ to $Z' \rightarrow b\bar{b}$.

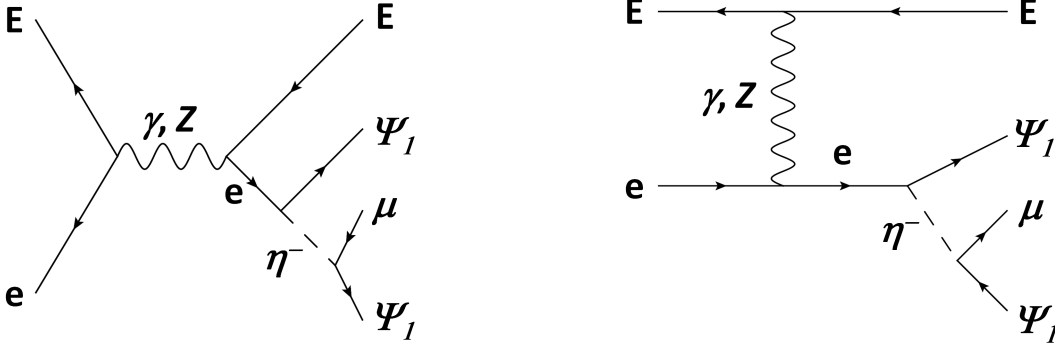


FIG. 1: Feynman diagrams for the signal process of the dark matter.

C. Detectability of right-handed neutrino

The right-handed neutrinos would be produced via the decay of the Z' at the LHC:

$$q\bar{q} \rightarrow Z' \rightarrow \nu_R \bar{\nu}_R. \quad (8)$$

In our model, if the decay of right-handed neutrinos into the dark matter and a SM singlet scalar s_1^0 is kinematically forbidden, the possible decay of the right-handed neutrinos is $\nu_R \rightarrow \ell^\pm W^\mp$. In this case, detectability of the right-handed neutrinos at the LHC has been studied in the simplest $U(1)_{B-L}$ model in Refs. [29, 32]. For example, the right-handed neutrinos can be detected at 26.3σ C.L. with $M_R = 200$ GeV, $m_{Z'} = 1.5$ TeV and $g_{B-L} = 0.2$ at the LHC with $\sqrt{s} = 14$ TeV and 100 fb^{-1} [29].

IV. PHYSICS AT THE ILC

We here consider testability of our radiative type-I seesaw model at the ILC. It is difficult to detect signals of the model at the LHC if the $U(1)_{B-L}$ gauge boson Z' is too heavy to be produced. Even for the case, the ILC can test the dark matter, right-handed neutrinos and the scalar sector.

A. Detectability of dark matter

In our model, the mass of the dark matter is about a half of the SM-like Higgs boson mass ($m_{h^0}/2$ or $m_{H^0}/2$) to satisfy the WMAP data. The dark matter directly couples to charged leptons. We concentrate on the process $e^+e^- \rightarrow e^+\Psi_1\eta^- \rightarrow e^+\mu^-\Psi_1\bar{\Psi}_1$, where η^- is an on-shell state, depicted in Fig. 1. The dark matter can be detected as missing particles by using the energy momentum conservation for the process.

We assume $\sqrt{s} = 350$ GeV and $\sqrt{s} = 500$ GeV at the ILC. The outgoing electron tends to be emitted to forward and backward directions because this is a t -channel process. Therefore, the detectability of the leptons near the beam line is important. We assume that detectable regions of the scatter angle (θ_ℓ) of the emitted lepton are given for $\sqrt{s} = 350$ GeV and $\sqrt{s} = 500$ GeV by $|\cos(\theta_\ell)| < 0.99955$ and $|\cos(\theta_\ell)| < 0.9998$, respectively [37].

The background processes are charged lepton flavor changing ones with missing momenta such as $e^+e^- \rightarrow e^+W^-\nu_e \rightarrow e^+\mu^-\nu_e\bar{\nu}_\mu$. In order to increase signal significance, we impose kinematical cuts for the case with $\sqrt{s} = 350$ GeV as follows:

$$\begin{aligned} 0.96 < |\cos(\theta_\ell)| < 0.99955, \quad \cos(\theta_{e\mu}) < 0, \quad M_{e\mu} < 80 \text{ GeV}, \\ E_e < 30 \text{ GeV}, \quad E_\mu > 100 \text{ GeV}, \quad 120 \text{ GeV} < M_{miss} < 190 \text{ GeV}, \end{aligned} \quad (9)$$

where $\theta_{e\mu}$, $M_{e\mu}$, E_ℓ and M_{miss} are the angle between electron and muon, invariant mass of electron and muon, energy of ℓ and missing invariant mass, respectively. The following cuts are imposed for the case with $\sqrt{s} = 500$ GeV:

$$\begin{aligned} 0.98 < |\cos(\theta_e)| < 0.9998, \quad |\cos(\theta_\mu)| < 0.8, \quad |\cos(\theta_{e\mu})| < 0.8 \\ E_e < 120 \text{ GeV}, \quad E_\mu > 80 \text{ GeV}, \quad M_{miss} > 120 \text{ GeV}. \end{aligned} \quad (10)$$

We show the detectability of the dark matter after applying all cuts for $\sqrt{s} = 350$ GeV and $\sqrt{s} = 500$ GeV in left and right panels of Fig. 2, respectively. The vertical axis is the cross section and the horizontal axis is the dark matter mass. All parameters but M_{Ψ_1} are set to the values in Table II. The red (solid) line and the green (dashed) line represent signal and background cross sections, respectively. The blue (dotted) line means the cross section for which the signal significance ($N_S/\sqrt{N_B}$ where N_S and N_B are number of events for signal and backgrounds) is 3 with 1 ab^{-1} . The left panel of Fig. 2 show that the dark matter can be detected at the ILC with $\sqrt{s} = 350$ GeV and 1 ab^{-1} for $M_{\Psi_1} \lesssim 64$ GeV at 3σ C.L. In the right panel of Fig. 2, we find that the dark matter can be detected for $M_{\Psi_1} \lesssim 80$ GeV at the ILC with $\sqrt{s} = 500$ GeV and 1 ab^{-1} at more than 3σ C.L.

The cross section of the signal process depends on the mass of η^\pm . In left and right panels of Fig. 3, we show the dependence of the signal cross section on m_{η^\pm} after applying all cuts for $\sqrt{s} = 350$ GeV and $\sqrt{s} = 500$ GeV, respectively. Parameters but m_{η^\pm} are set on the values in Table II. Meanings of all of lines the same as those in Fig. 2. The dark matter would be detected at the ILC with $\sqrt{s} = 350$ GeV and $\sqrt{s} = 500$ GeV for $m_{\eta^\pm} \lesssim 280$ GeV and $m_{\eta^\pm} \lesssim 380$ GeV, respectively.

If the decay of the SM-like Higgs bosons into the dark matter is kinematically allowed, its branching ratios are $\mathcal{O}(1)\%$. In this case, dark matter would be detected at the ILC with $\sqrt{s} = 350$ GeV [35]. Furthermore, direct detection experiments of dark matter are

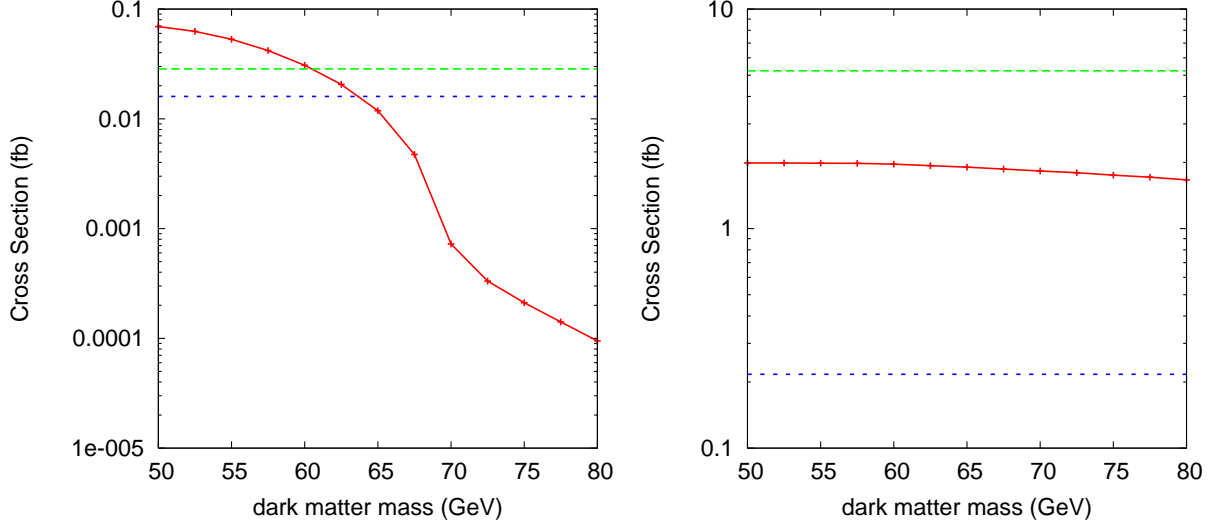


FIG. 2: The cross section of signal of the dark matter at the ILC with $\sqrt{s} = 350$ GeV (left) and $\sqrt{s} = 500$ GeV (right). The red (solid) line and the green (dashed) lines are signal and background cross section, respectively. The blue (dotted) line means the limit that the signal significance $N_S/\sqrt{N_B} = 3$ with 1 ab^{-1} .

very important for our model. Since the annihilation cross section of Ψ_1 is proportional to v_σ^{-2} , the dark matter abundance becomes inconsistent with the WMAP data [9] if $v_\sigma \gtrsim 16$ TeV. Therefore, the spin independent scattering cross section between dark matter and neutron via Z' boson is more than $2 \times 10^{-47} \text{ cm}^2$, and this signal could be detected at the XENON1T [36]. If dark matter mass measured at direct detection experiments is consistent with m_{Ψ_1} measured at the ILC, the Ψ_1 would be identified as dark matter. In this case, the lepton flavor changing process of $e^+e^- \rightarrow e^+\Psi_1\eta^- \rightarrow e^+\mu^-\Psi_1\bar{\Psi}_1$ indicates that the dark matter is directly coupled to charged leptons. Moreover, if we utilize the beam polarization, it could be checked that the dark matter only couples with left-handed leptons. That kind of the dark matter would contribute to neutrino mass generation mechanism.

Notice that $e^+e^- \rightarrow e^+\Psi_1\eta^- \rightarrow e^+\tau^-\Psi_1\bar{\Psi}_1$ process would be also useful to detect the dark matter because the $f_{\mu 1}$ coupling constant is constrained by $\mu \rightarrow e\gamma$ while the $f_{\tau 1}$ coupling constant is not strictly constrained. Therefore, the cross section for the τ mode tends to be larger than the one for the μ mode. If the dark matter can be detected in both μ and τ modes, we test the ratio between $f_{\mu 1}$ and $f_{\tau 1}$.

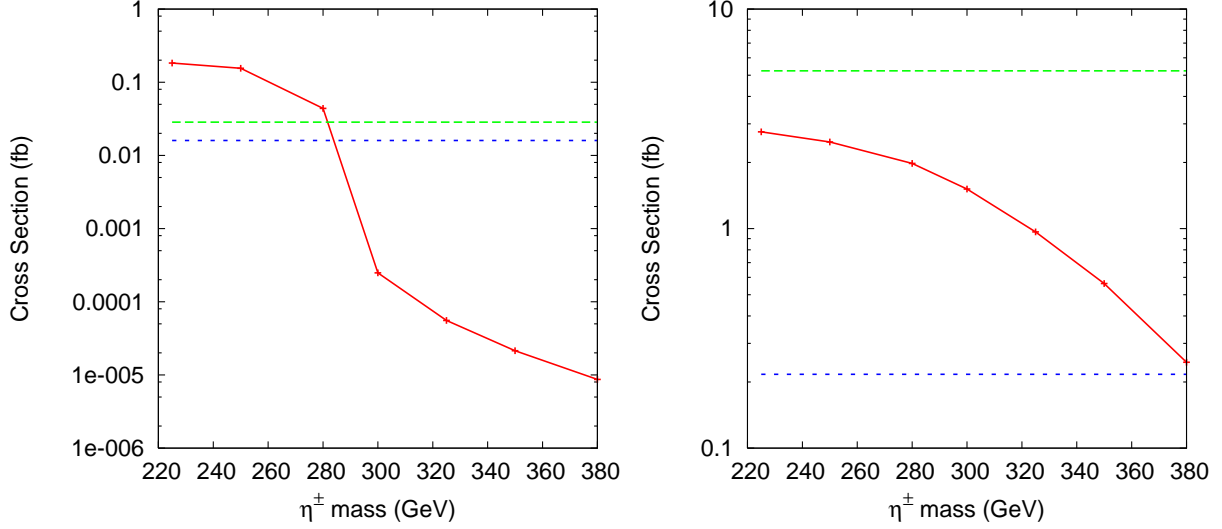


FIG. 3: The dependence of the signal cross section on mass of the η^\pm at the ILC with $\sqrt{s} = 350$ GeV (left) and $\sqrt{s} = 500$ GeV (right). Meanings of all of lines are the same as those in Fig. 2.

B. Detectability of right-handed neutrinos

Next, we consider detectability of right-handed neutrinos at the ILC. In our model, neutrino Dirac Yukawa and SM gauge coupling constants of right-handed neutrinos are not large. However, right-handed neutrinos couple to $U(1)_{DM}$ charged particles such as Ψ_2 with sizable coupling constants of $\mathcal{O}(0.1)$. In this case, right-handed neutrinos can be produced via Ψ_2 . We concentrate on the process, $e^+e^- \rightarrow \Psi_1 \bar{\Psi}_2 \rightarrow \Psi_1 \bar{\nu}_R s_1^0 \rightarrow \Psi_1 W^- \ell^+ s_1^0$ where ℓ is electron and muon, depicted in Fig. 4. We use the two-jet mode of the W boson decay while s_1^0 decays invisibly into Ψ_1 and left-handed neutrinos.

In our choice of the parameters of the model, the center of mass energy around 1 TeV is necessary to produce Ψ_2 at the ILC. We here consider the case with $\sqrt{s} = 1$ TeV for right-handed neutrino detection via $\Psi_2 \rightarrow s_1^0 \nu_R$. Main background process is $e^+e^- \rightarrow W^- \ell^+ \nu_i \gamma$ with photon missing events. We impose the following kinematical cuts in order to increase signal significance:

$$\begin{aligned}
& |\cos(\theta_\ell)| < 0.95, \quad 200 \text{ GeV} < M_{miss} < 600 \text{ GeV}, \\
& 0.9999416 < |\cos(\theta_\gamma)|, \\
& 240 \text{ GeV} < M_{W\ell} < 260 \text{ GeV}, \quad E_\ell < 300 \text{ GeV}, \\
& 300 \text{ GeV} < E_{W\ell} < 600 \text{ GeV},
\end{aligned} \tag{11}$$

where θ_x represent the scattering angle of the particle x , and $E_{W\ell}$ and $M_{W\ell}$ are the energy and the invariant mass between the W boson and ℓ , respectively.

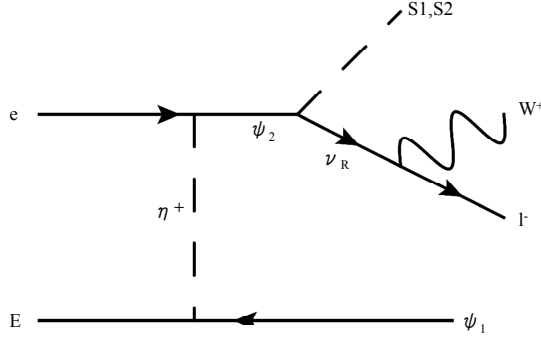


FIG. 4: Feynman diagram of the signal process of right-handed neutrinos.

In Fig. 5, we show the detectability of right-handed neutrinos after applying all cuts. The horizontal axis is $\sqrt{f_{e1}f_{e2}}$ and the other parameters are set on values in Table II. The red (solid) line and the green (dashed) line are signal and background cross section times $\text{BR}(W \rightarrow jj)$, respectively. Cross sections for which the signal significance ($N_S/\sqrt{N_B}$) becomes 3 are presented with the blue (dotted) line for 1 ab^{-1} and the magenta (dash-dotted) line for 3 ab^{-1} . In Fig. 5, we find that right-handed neutrinos can be detected at the 3σ C.L. at the ILC with $\sqrt{s} = 1 \text{ TeV}$ and 3 ab^{-1} in our parameter set. If $M_R > M_{\Psi_1} + m_{s_1^0}$, right-handed neutrinos can decay into $U(1)_{DM}$ charged particles. In this case, $\nu_R \rightarrow \Psi_1 s_1^0$ is the main decay mode of right-handed neutrinos. Therefore most of right-handed neutrinos decay into $U(1)_{DM}$ charged particles invisibly, and it is difficult to detect right-handed neutrinos.

C. Scalar sector

Two SM-like CP-even Higgs bosons (h^0 and H^0) with the large mixing are predicted in our model. If the 125 GeV boson discovered at the LHC is identified to the SM-like Higgs boson, it means that both of masses of h^0 and H^0 are close to this signal mass in our model. The energy resolution for the Higgs boson is expected to be better than about 50 MeV at the ILC [28]. Therefore, two CP-even Higgs bosons would be separated at the ILC. Notice that there is no CP-odd scalar boson without $U(1)_{DM}$ charge in this model. On the other hand, charged scalar bosons η^\pm dominantly decay into left-handed charged lepton and dark matter. This decay process is similar to slepton decay in super symmetric models. If η^\pm are produced in pair at TeV-scale colliders, m_{η^\pm} would be reconstructed using the maximum M_{T2} value [38] or lepton energy distribution [39].

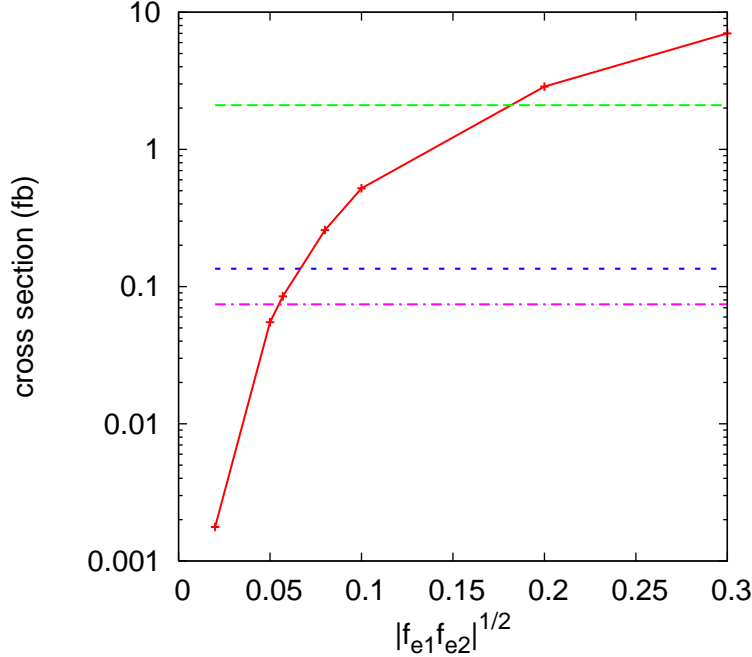


FIG. 5: Right-handed neutrino detectability at the $\sqrt{s} = 1$ TeV ILC. The red (solid) line and the green (dashed) line are signal and background cross section times $\text{BR}(W \rightarrow jj)$. The blue (dotted) and magenta (dash-dotted) lines mean the limit that the signal significance ($N_S/\sqrt{N_B}$) are three with 1 ab^{-1} and 3 ab^{-1} , respectively.

V. CONCLUSIONS

We have investigated testability of the TeV-scale radiative type-I seesaw model at TeV-scale colliders, which explains tiny neutrino masses, the fermionic dark matter mass and the stability of the dark matter by introducing the $U(1)_{B-L}$ gauge symmetry. We have found that the dark matter could be detected with the mass up to about 64 GeV with the integrated luminosity 1 ab^{-1} at the ILC with $\sqrt{s} = 350$ GeV. The allowed region of the dark matter mass would be probed at the ILC with $\sqrt{s} = 500$ GeV. Since the value of v_σ is less than about 16 TeV for consistency with the WMAP data, dark matter direct detection experiments also could cover this region. Right-handed neutrinos could be discovered at the ILC with $\sqrt{s} = 1$ TeV and 1 ab^{-1} if the invisible decay $\nu_R \rightarrow \Psi_1 s_1^0$ is kinematically forbidden. Therefore, the model has sufficient possibilities to be distinguished from the other models by combination with dark matter search experiments and TeV-scale colliders such as the LHC and the ILC.

Acknowledgments

This work of S.K. was supported in part by Grant-in-Aid for Scientific Research, Nos. 22244031 , 23104006 and 24340046. The work of H.S. was supported in part by the Grant-in-Aid for Young Scientists (B) No. 23740210. The work of T.N. was supported in part by the Japan Society for the Promotion of Science as a research fellow (DC2).

-
- [1] S. Kanemura, T. Nabeshima and H. Sugiyama, Phys. Rev. D **85**, 033004 (2012)
 - [2] B. T. Cleveland *et al.*, Astrophys. J. **496**, 505 (1998); W. Hampel *et al.* [GALLEX Collaboration], Phys. Lett. B **447**, 127 (1999); B. Aharmim *et al.* [SNO Collaboration], Phys. Rev. Lett. **101**, 111301 (2008); J. N. Abdurashitov *et al.* [SAGE Collaboration], Phys. Rev. C **80**, 015807 (2009); K. Abe *et al.* [Super-Kamiokande Collaboration], Phys. Rev. D **83**, 052010 (2011); G. Bellini *et al.* [Borexino Collaboration], Phys. Rev. Lett. **107**, 141302 (2011).
 - [3] R. Wendell *et al.* [Kamiokande Collaboration], Phys. Rev. D **81**, 092004 (2010).
 - [4] M. H. Ahn *et al.* [K2K Collaboration], Phys. Rev. D **74**, 072003 (2006); P. Adamson *et al.* [The MINOS Collaboration], Phys. Rev. Lett. **106**, 181801 (2011).
 - [5] K. Abe *et al.* [T2K Collaboration], Phys. Rev. Lett. **107**, 041801 (2011).
 - [6] M. Apollonio *et al.* [CHOOZ Collaboration], Eur. Phys. J. C **27**, 331 (2003); Y. Abe *et al.* [DOUBLE-CHOOZ Collaboration], Phys. Rev. Lett. **108**, 131801 (2012); F. P. An *et al.* [DAYA-BAY Collaboration], Phys. Rev. Lett. **108**, 171803 (2012); J. K. Ahn *et al.* [RENO Collaboration], Phys. Rev. Lett. **108**, 191802 (2012).
 - [7] A. Gando *et al.* [The KamLAND Collaboration], Phys. Rev. D **83**, 052002 (2011).
 - [8] F. Zwicky, Helv. Phys. Acta **6**, 110 (1933).
 - [9] D. Larson *et al.*, Astrophys. J. Suppl. **192**, 16 (2011).
 - [10] A. D. Sakharov, Pisma Zh. Eksp. Teor. Fiz. **5**, 32 (1967) [JETP Lett. **5**, 24 (1967)] [Sov. Phys. Usp. **34**, 392 (1991)] [Usp. Fiz. Nauk **161**, 61 (1991)].
 - [11] P. Minkowski, Phys. Lett. B **67**, 421 (1977); T. Yanagida, in Proceedings of the “*Workshop on the Unified Theory and the Baryon Number in the Universe*”, Tsukuba, Japan, Feb. 13-14, 1979, edited by O. Sawada and A. Sugamoto, KEK report KEK-79-18, p. 95; Prog. Theor. Phys. **64**, 1103 (1980); M. Gell-Mann, P. Ramond and R. Slansky, in “*Supergravity*” eds. D. Z. Freedman and P. van Nieuwenhuizen, (North-Holland, Amsterdam, 1979); R. N. Mohapatra and G. Senjanovic, Phys. Rev. Lett. **44**, 912 (1980).
 - [12] P. H. Gu and U. Sarkar, Phys. Rev. D **77**, 105031 (2008).
 - [13] L. M. Krauss, S. Nasri and M. Trodden, Phys. Rev. D **67**, 085002 (2003); K. Cheung and

- O. Seto, Phys. Rev. D **69**, 113009 (2004).
- [14] E. Ma, Phys. Rev. D **73**, 077301 (2006); Phys. Lett. B **662**, 49 (2008); T. Hambye, K. Kannike, E. Ma and M. Raidal, Phys. Rev. D **75**, 095003 (2007); E. Ma and D. Suematsu, Mod. Phys. Lett. A **24**, 583 (2009).
- [15] E. Ma, Mod. Phys. Lett. A **23**, 721 (2008).
- [16] M. Aoki, S. Kanemura and O. Seto, Phys. Rev. Lett. **102**, 051805 (2009); Phys. Rev. D **80**, 033007 (2009); M. Aoki, S. Kanemura and K. Yagyu, Phys. Rev. D **83**, 075016 (2011); Phys. Lett. B **702**, 355 (2011).
- [17] S. Kanemura, T. Nabeshima and H. Sugiyama, Phys. Lett. B **703**, 66 (2011).
- [18] S. Kanemura and H. Sugiyama, arXiv:1202.5231 [hep-ph].
- [19] S. S. C. Law and K. L. McDonald, arXiv:1204.2529 [hep-ph].
- [20] Y. Farzan and E. Ma, arXiv:1204.4890 [hep-ph].
- [21] H. Okada and T. Toma, arXiv:1207.0864 [hep-ph].
- [22] S. Kanemura and T. Ota, Phys. Lett. B **694**, 233 (2010) [arXiv:1009.3845 [hep-ph]].
- [23] D. Suematsu and T. Toma, Nucl. Phys. B **847**, 567 (2011).
- [24] S. Kanemura, O. Seto and T. Shimomura, Phys. Rev. D **84**, 016004 (2011).
- [25] M. Lindner, D. Schmidt and T. Schwetz, Phys. Lett. B **705**, 324 (2011).
- [26] P. Mal [ATLAS Collaboration], arXiv:1206.1174 [hep-ex];
The ATLAS Collaboration, ATLAS-CONF-2012-093.
- [27] M. Pieri [CMS Collaboration], arXiv:1205.2907 [hep-ex];
The CMS Collaboration, CMS PAS HIG-12-020.
- [28] T. Abe *et al.* [ILD Concept Group - Linear Collider Collaboration], arXiv:1006.3396 [hep-ex].
- [29] L. Basso, A. Belyaev, S. Moretti and C. H. Shepherd-Themistocleous, Phys. Rev. D **80**, 055030 (2009); L. Basso, A. Belyaev, S. Moretti, G. M. Pruna and C. H. Shepherd-Themistocleous, Eur. Phys. J. C **71**, 1613 (2011).
- [30] J. Brau, (Ed.) *et al.* [ILC Collaboration], arXiv:0712.1950 [physics.acc-ph]; G. Aarons *et al.* [ILC Collaboration], arXiv:0709.1893 [hep-ph]; N. Phinney, N. Toge and N. Walker, arXiv:0712.2361 [physics.acc-ph]; T. Behnke, (Ed.) *et al.* [ILC Collaboration], arXiv:0712.2356 [physics.ins-det].
- [31] The CLIC Study Team, "A 3 TeV e^+e^- Linear Collider based on CLIC Technology", CERN 2000-008, Proton Synchrotron Division, July 28, 2000; E. Accomando *et al.* [CLIC Physics Working Group Collaboration], hep-ph/0412251.
- [32] H. Mansour and N. Bakhiet, arXiv:1206.4533 [nucl-th];
H. Mansour and N. Bakhiet, arXiv:1206.4534 [nucl-th].
- [33] J. Erler, P. Langacker, S. Munir and E. Rojas, JHEP **1111**, 076 (2011)

- [34] E. E. Jenkins, Phys. Lett. B **192**, 219 (1987).
- [35] M. Schumacher, LC-PHSM-2003-096.
- [36] E. Aprile [XENON1T Collaboration], arXiv:1206.6288 [astro-ph.IM].
- [37] H. Abramowicz, A. Abusleme, K. Afanaciev, J. Aguilar, P. Ambalathankandy, P. Bambade, M. Bergholz and I. Bozovic-Jelisavcic *et al.*, JINST **5**, P12002 (2010) [arXiv:1009.2433 [physics.ins-det]].
- [38] C. G. Lester and D. J. Summers, Phys. Lett. B **463**, 99 (1999).
- [39] S. Kawabata, Y. Shimizu, Y. Sumino and H. Yokoya, Phys. Lett. B **710**, 658 (2012).